10.1071/CH17354_AC

Australian Journal of Chemistry 2018, 71(2 & 3), 87-94

SUPPLEMENTARY MATERIAL

Ultrafast NH_3 Sensing Properties of WO_3@$CoWO_4$ Heterojunction Nanofibres at Room Temperature

Yiming Zhao,[A] *Muhammad Ikram,*[A] *Jianzhou Wang,*[A] *Zhi Liu,*[A] *Lijuan Du,*[E] *Jiao Zhou,*[A] *Kan Kan,*[C] *Weijun Zhang,*[D] *Li Li*[A,B,F] and *Keying Shi*[A,F]

[A] Key Laboratory of Functional Inorganic Material Chemistry, Ministry of Education, School of Chemistry and Material Science, Heilongjiang University, Harbin, 150080, China.

[B] Key Laboratory of Chemical Engineering Process & Technology for High-efficiency Conversion, Heilongjiang University, Harbin, 150080, China.

[C] Daqing Branch, Heilongjiang Academy of Sciences, Daqing 163319, China.

[D] Institute of Advanced Technology, Heilongjiang Academy of Sciences, Harbin 150020, China.

[E] Modern Experiment Center, Harbin Normal University, Harbin 150025, China.

[F] Corresponding authors. E-mail: shikeying2008@163.com; llwjjhlju@sina.cn

Fax: +86 4518667 3647; Tel: +86 451 8660 9141.

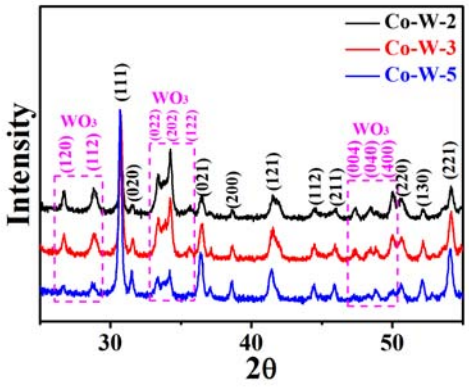

Figure S1. XRD patterns of Figure 1a with 2θ ranged from 25 to 55.

In Figure S1, the peaks at about 26.59, 28.92, 35.66, 47.24, 48.24 and 49.93 degrees were aimed to peaks (120), (112), (122), (004), (040) and (400) of WO_3, and about 31.43, 36.39, 38.52, 41.45, 44.33, 45.79, 50.53, 52.02 and 54.12 degrees were aimed to peaks (020), (021), (200), (121), (112),(211), (220), (130) and (221) of $CoWO_4$.

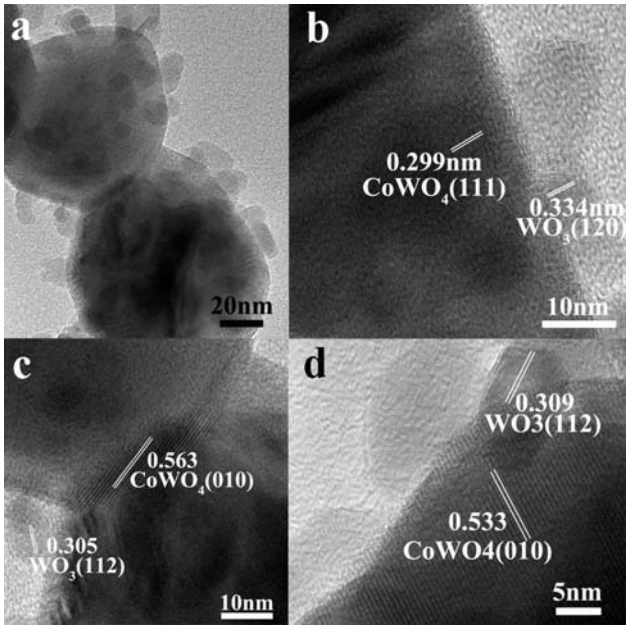

Figure S2. TEM images of Co-W-2.

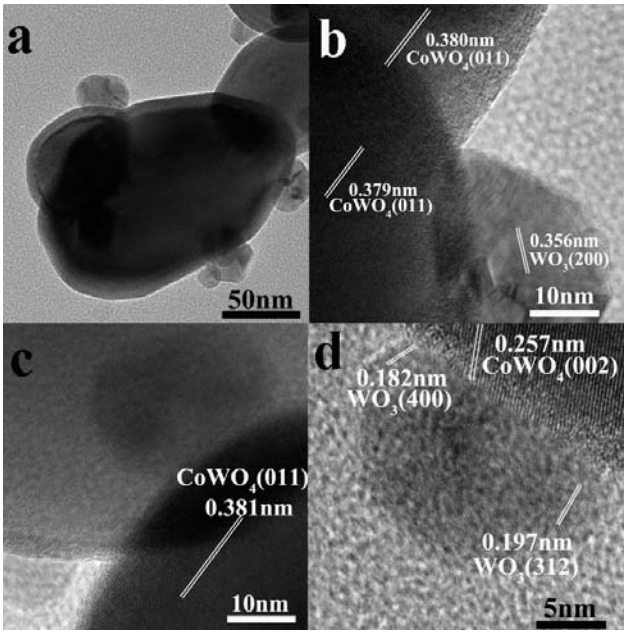

Figure S3. TEM images of Co-W-5.

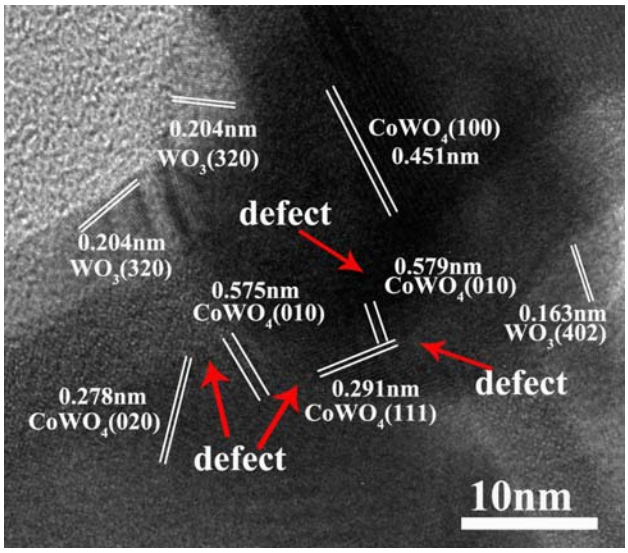

Figure S4. TEM image of Co-W-3, showing $CoWO_4$-WO_3 p-n heterojunctionand $CoWO_4$-$CoWO_4$ p-p homojunction.

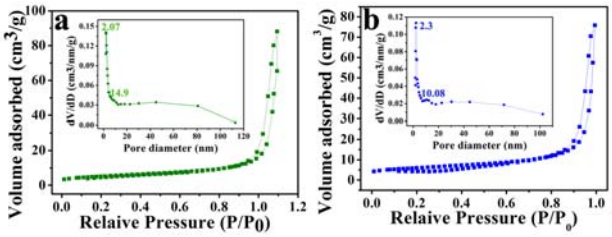

Figure S5. N_2 adsorption–desorption isotherms and pore-size distribution curves (the inset) of (a) Co-W-2 and (b) Co-W-5.

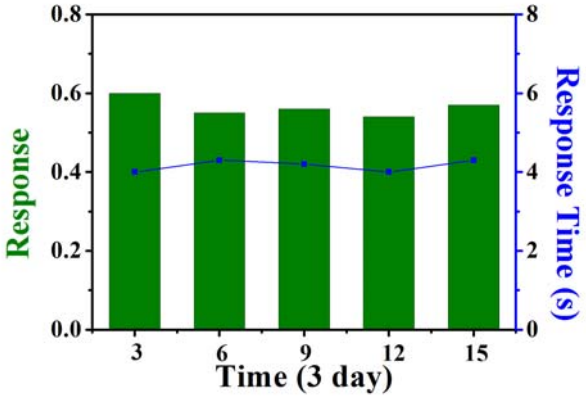

Figure S6. The response of the Co-W-3 for 15 days with 100ppm NH_3 at RT.

Table S1. O 1s peak position and peak area ratio of the four samples

Sample	WO_3		Co-W-2			Co-W-3			Co-W-5		
Peak	O_1	O_2	O_1	O_2	O_3	O_1	O_2	O_3	O_1	O_2	O_3
Peak position(eV)	529.9	531.0	529.9	530.5	532.0	529.8	**530.5**	**531.8**	529.9	**530.5**	**531.9**
Peak area ratio(%)	71.9	28.1	51.4	22.1	26.5	41.9	**20.5**	**37.6**	37.3	**28.4**	**34.3**

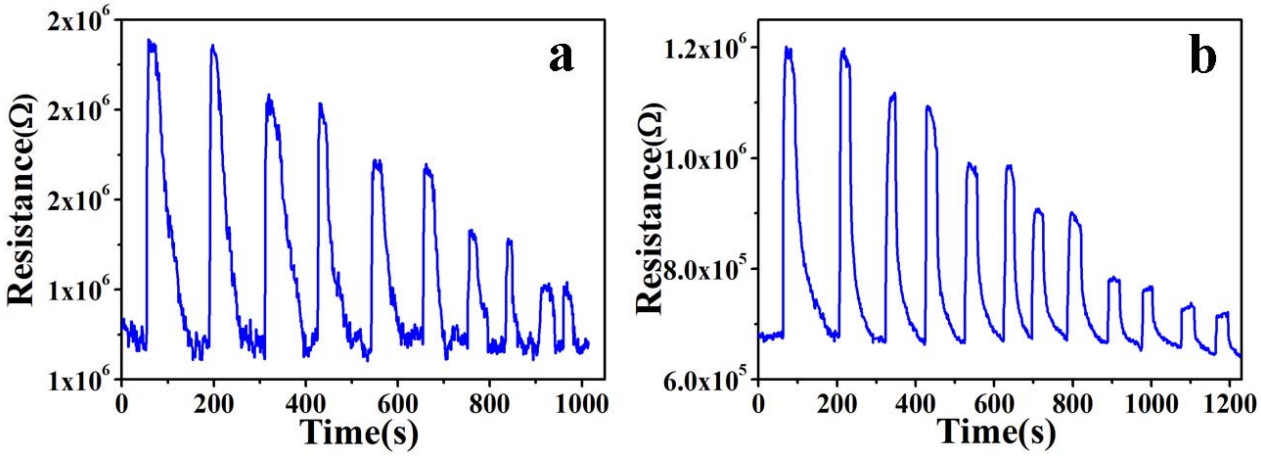

Figure S7. Dynamic response-recovery curves of samples. (a) Co-W-2, (b) Co-W-5 (RH: 26%).

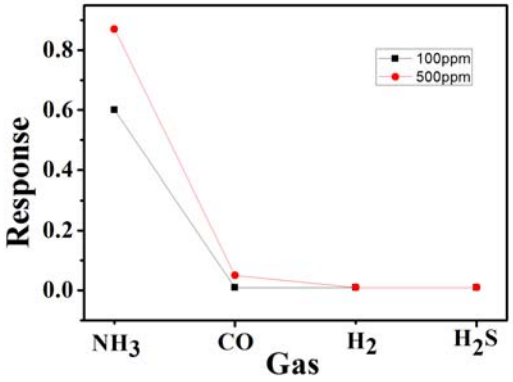

Figure S8. Gas selectivity chart of Co-W-3 sample with different concentration of gas.

We had injection 500 and 100ppm different kinds of gas. For 500ppm, the response to NH_3 was 0.87, and to CO was 0.05, to other two gas had no response; to 100ppm, the response to NH_3 was 0.6, but the response to CO had no response like other two gas. So that it could show the excellent gas selectivity for NH_3

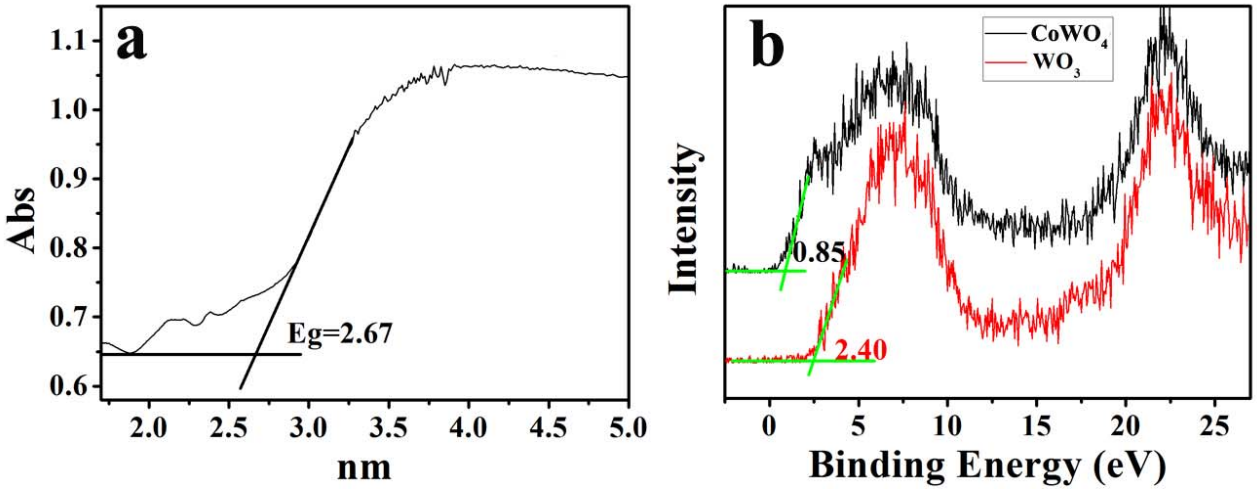

Figure S9. (a) The Eg value of $CoWO_4$ and (b) the valence band spectrum of WO_3 and $CoWO_4$.

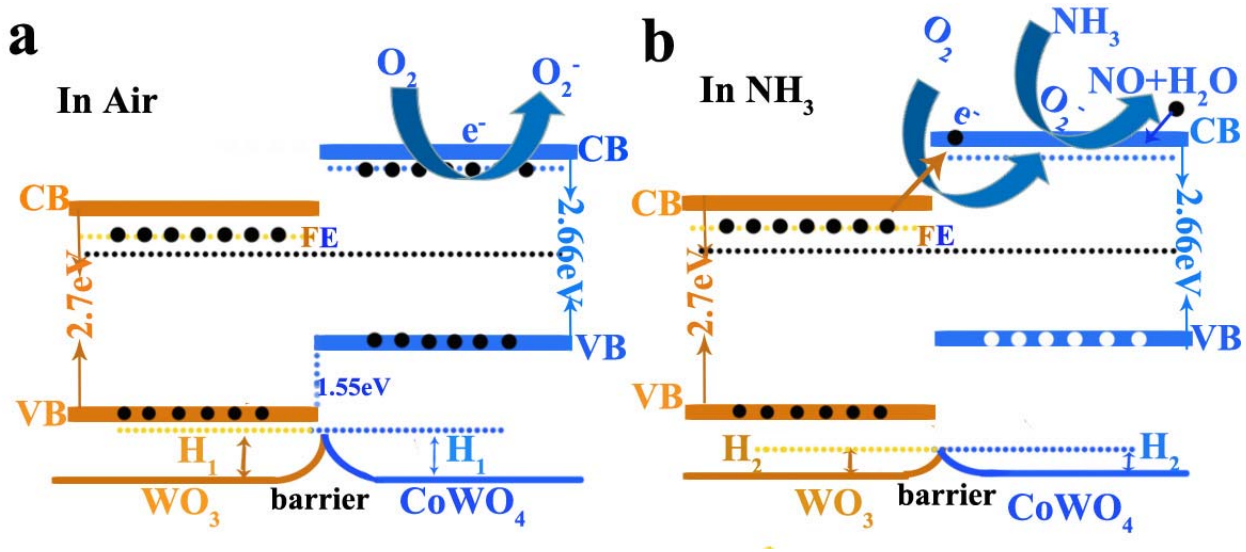

Figure S10. Schematic illustrations of gas sensing: energy band diagrams and the corresponding interfacial potential barrier heights (a) in air; (b) in NH_3

Table S2: The response and response time of WO_3 and WO_3-$CoWO_4$ sensor to different NH_3 concentrations at room temperature

Sample	cycle number	concentration (ppm)	1000	500	100	50	10	5
WO_3	1	Response	-	-	-	-	-	-
		Response time	-	-	-	-	-	-

		(s)						
		Response	0.25	0.21	0.15	0.09	0.05	-
	1	Response time (s)	4.3	4.6	5.3	5.3	6.0	-
Co-W-2		Response	0.24	0.20	0.15	0.09	0.05	-
	2	Response time (s)	4.6	4.8	4.6	5.3	5.7	-
		Response	1.17	0.93	0.60	0.38	0.24	-
	1	Response time (s)	3.0	3.3	4.0	4.3	4.6	-
Co-W-3		Response	1.19	0.83	0.57	0.40	0.25	-
	2	Response time (s)	3.6	4.3	4.0	4.3	4.6	-
		Response	0.77	0.64	0.45	0.34	0.15	0.07
	1	Response time (s)	2.0	2.6	3.0	3.3	3.7	4.0
Co-W-5		Response	0.76	0.62	0.45	0.33	0.12	0.06
	2	Response time (s)	2.7	3.0	3.6	3.3	3.6	4.0

Table S3. Comparison of the sensing performances of our proposed NH_3 sensor with those reported in the literature

Material	NH_3(ppm)	Sensor response	Temperature(□)	Response time (s)	References
ZnO/WO_3	100	1.69(Ra/Rg)	RT	-	1.
Pt/WO_3	100	12(Rg/Ra)	125	-	2.
WO_3	100	5.5(Ra/Rg)	500	1	3.

WO_3 NFs	100	5.5(Rg/Ra)	200	-	4.
WO_3-$CoWO_4$	100	0.6(ΔRg/Ra)	RT	4	Present work

Table S4. The BET surface and pore size of the three samples.

sample	BET surface (m^2/g)	Pore size (nm)
Co-W-2	37.27	2.07, 14.9
Co-W-3	38.35	2.1, 15.1
Co-W-5	36.82	2.3, 10.8

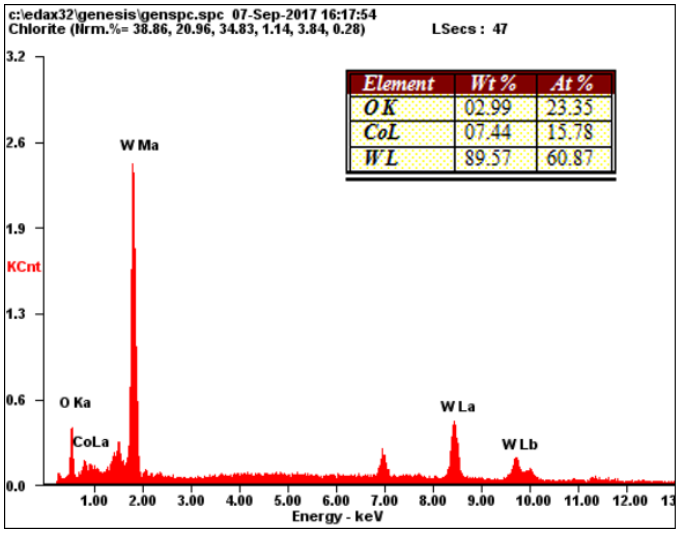

Figure S11. The EDS of Co-W-3.

Table S5. Comparison of the sensing performances of NH_3 sensors at room temperature

Material	NH_3(ppm)	Sensor response	Temperature(℃)	Response time (s)	References
WS_2	250	2.5	RT	200	5.
ZnO-PANI	100	1.3	RT	21	6.
Plasma CNTS	100	22.5%	RT	60	7.
PANI -Fe_2O_3	100	72%	RT	50	8.
PANI-WO_3	100	1.5	RT	39	9
MoS_2-ZnO	50	45%	RT	10	10
CVD graphene	1300	1.5	RT	156	11
WO_3-$CoWO_4$	100	60%	RT	4	Present work

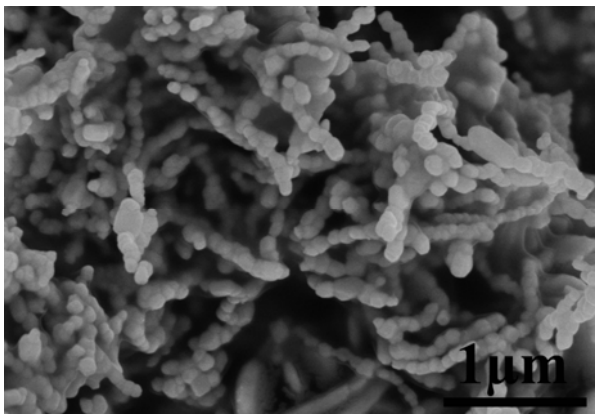

Figure S12. The SEM of Co-W-3.

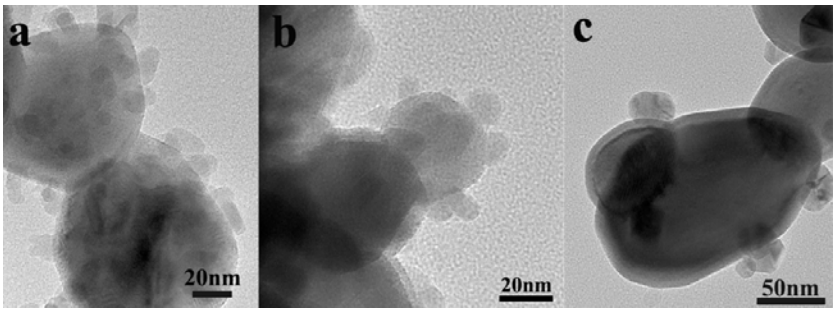

Figure S13: HRTEM images of (a) Co-W-2; (b) Co-W-3; (c) Co-W-5**.**

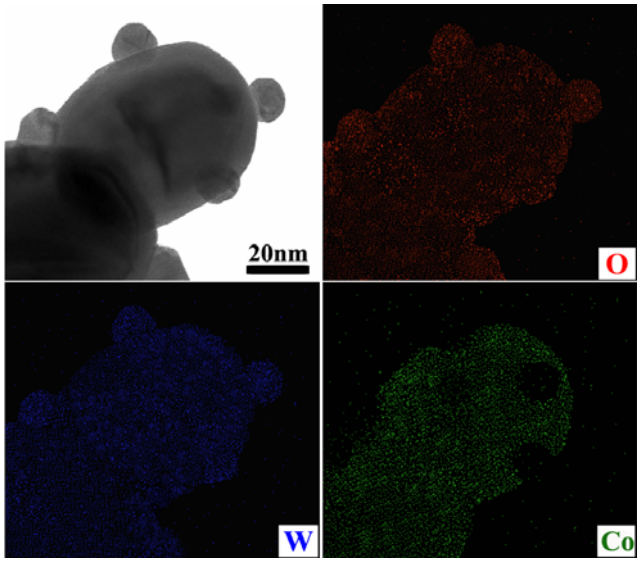

Fig. S14. EDS mapping of the sample Co-W-3: (a) TEM image; (b–d) corresponding to O, W and Co elemental mapping, respectively.

References:

1. N. M. Vuong; N. D. Chinh; T. T. Hien; N. D. Quang; D. Kim; H. J. Kim; S. G. Yoon; D. Kim, *J. Nanosci. Nanotechnol.*, **2016**, *16*, 10346–10350.

2. Y. L. Wang; J. Liu; X. B. Cui; Y. Gao; J. Ma; Y. F. Sun; P. Sun; F. M. Liu; X. S. Liang; T. Zhang; G. Y. Lu, *Sens. Actuators, B*, **2017**, *238*, 473–481.

3. J. Y. Leng; X. J. Xu; N. Lv; H. T. Fan; T. Zhang, *J. Colloid Interface Sci.*, **2011**, *356*, 54–57.

4. J. Leng; X. Xu; N. Lv; H. Fan; T. Zhang, *J. Colloid Interface Sci.*, **2010**, *356*, 54–57.

5. Z.Y. Qin; D.W. Zeng; J. Zhang; C.Y. Wu; Y.W. Wen; B. Shan; C.S. Xie, *Applied Surface Science*, **2017**, 414, 244–250
6. M. Das; D. Sarkar, *Ceramics International*, **2017**, 43, 11123–11131
7. A. G. Bannov; O. Jašek; A. Manakhov; M. Márik; D. Neˇcas; L. Zajíˇcková, *IEEE. SENS. J.*, **2017**, 17, 1964-1970.
8. D.K. Bandgar; S.T. Navale; Y.H. Navale; S.M. Ingole; F.J. Stadler; N. Ramgir; D.K. Aswal; S.K. Gupta; R.S. Mane; V.B. Patil, *Materials Chemistry and Physics*, **2017**, 189, 191-197.
9. S.B. Kulkarni; Y.H. Navale; S.T. Navale; N.S. Ramgir; A.K. Debnath; S.C. Gadkari; S.K. Gupta; D.K. Aswal; V.B. Patil, *Organic Electronics*, **2017**, 45, 65-73.
10. D.Z. Zhang; C.X. Jiang; Y.E. Sun, *Journal of Alloys and Compounds*, **2017,** 698, 476-483.
11. C. S. Yang; A. Mahmood; B. Kim; K. Shin; D. H. Jeon; J. K. Han; S. D. Bu; S. Park; W. J. Choi; B. Doudin, *2D Mater.*, **2016**, 3, 011007.